Electronic Supplementary Material (ESI) for Dalton Transactions.

Supporting Information

Solution-phase decomposition of ferrocene into wüstite-iron oxide core-shell nanoparticles

M. J. Loedolff, R. O. Fuller, G. Nealon, M. Saunders, M. A. Spackman, G. A. Koutsantonis

Additional Experimental

Nuclear Magnetic Resonance

NMR Spectra were recorded on a Varian 400 MHz spectrometer (399.9 MHz for ^{1}H, 100.6 MHz for ^{13}C). Spectra were calibrated against the residual solvent signal of d6-benzene (δ 7.16 ppm for ^{1}H, 128.06 ppm for ^{13}C) and all chemical shifts are reported in ppm.

EDS Software information

Bruker Esprit V1.9 software was used for EDS quantification.

Nanoparticle Characterisation

SAED of spherical nanoparticles

Table S1 – Planar spacings measured from SAED patterns in Figures 2(b) and 2(d).

SAED Figure 2(b) label	SAED planar spacings from Figure 2(b) (nm)	SAED Figure 2(d) label	SAED planar spacings from Figure 2(d) (nm)	Planar spacings for Wüstite[1] (FeO) JCPDS No. 46-1412	Planar spacings for Magnetite[2] (Fe_3O_4) JCPDS No. 19-629	Planar spacings for Maghemite[3] (γ-Fe_2O_3) JCPDS No. 24-81
	-	i	0.295	-	2.9684	2.9513
i	0.249	ii	0.248	2.4863	2.5314	2.5168
ii	0.215	iii	0.214	2.1532	2.0989	2.0868
	-	iv	0.161	-	1.6158	1.6065
iii	0.151	v	0.151	1.5225	1.4842	1.4756
iv	0.130	vi	0.129	1.2984	1.2803	1.273
v	0.124	vii	0.124	1.2432	1.2118	1.2048

XRD of spherical nanoparticles

Table S2 – XRD data summarised for the spherical nanoparticles. Reflections correspond to wüstite[1] (FeO), magnetite[2] (Fe_3O_4) and/or maghemite[3] (γ-Fe_2O_3)), and iron[4] (α-Fe).

Position (°2θ)	Planar spacing (Å)	Relative Intensity (%)	Compound match	Miller Indices (hkl)
18.17	4.878	7.90	Fe_3O_4/γ-Fe_2O_3	111
29.99	2.977	27.24	Fe_3O_4/γ-Fe_2O_3	220
35.35	2.537	100.00	Fe_3O_4/γ-Fe_2O_3	311
36.00	2.493	52.00	FeO	111
36.99	2.428	5.18	Fe_3O_4/γ-Fe_2O_3	222
41.84	2.157	82.82	FeO	200
42.96	2.104	21.50	Fe_3O_4/γ-Fe_2O_3	400
44.58	2.031	37.98	Fe	110
53.32	1.717	9.19	Fe_3O_4/γ-Fe_2O_3	422
56.87	1.618	32.52	Fe_3O_4/γ-Fe_2O_3	511
60.67	1.525	35.62	FeO	220
62.47	1.486	43.75	Fe_3O_4/γ-Fe_2O_3	440
64.99	1.434	4.19	Fe	220
70.86	1.329	4.32	Fe_3O_4/γ-Fe_2O_3	620
72.55	1.302	12.19	FeO	311
72.79	1.298	12.44	Fe_3O_4/γ-Fe_2O_3	533
73.90	1.281	7.21	Fe_3O_4/γ-Fe_2O_3	622
76.42	1.245	8.83	FeO	222
82.22	1.172	6.61	Fe	211
89.56	1.094	10.54	Fe_3O_4/γ-Fe_2O_3	731

PDF card numbers for the phases presented in Table S2:

Fe_3O_4: JCPDS No. 19-629

γ-Fe_2O_3: JCPDS No. 24-81

FeO: JCPDS No. 46-1312

α-Fe: JCPDS No. 6-696

Exclusion of oleylamine from reaction solution

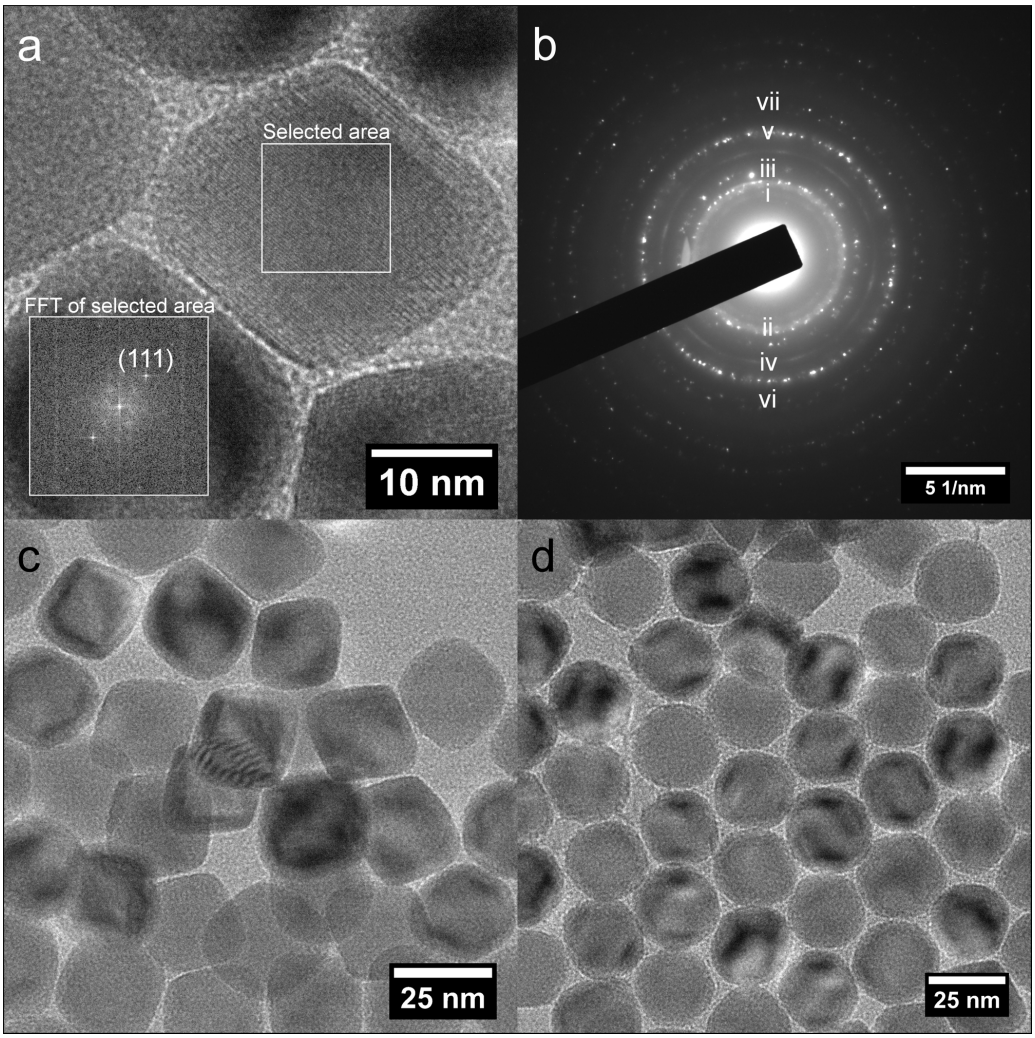

Figure S1 – TEM images of nanoparticles formed when oleylamine was excluded from the reaction mixture; (a) HRTEM image marked with a "selected area" with corresponding FFT inset corresponding to the (111) wüstite[1] (FeO) plane, (b) SAED pattern similar to that obtained from spherical NPs containing planar spacings consistent with wüstite[1] (FeO) and additional weak rings from magnetite[2] (Fe_3O_4) and/or maghemite[3] (γ-Fe_2O_3), (c) region with core-shell distorted cubic nanoparticles present in the sample and (d) region with core-shell spherical nanoparticles present.

Table S3 – Planar spacings measured from SAED pattern in Figure S1.

SAED Figure S1 label	SAED planar spacings (Å)	Planar spacings for Wüstite[1] (FeO) JCPDS No. 46-1412	Planar spacings for Magnetite[2] (Fe_3O_4) JCPDS No. 19-629	Planar spacings for Maghemite[3] (γ-Fe_2O_3) JCPDS No. 24-81
i	2.92	-	2.9684	2.9513
ii	2.49	2.4863	2.5314	2.5168
iii	2.14	2.1532	2.0989	2.0868
iv	1.59	-	1.6158	1.6065
v	1.52	1.5225	1.4842	1.4756
vi	1.30	1.2984	1.2803	1.273
vii	1.24	1.2432	1.2118	1.2048

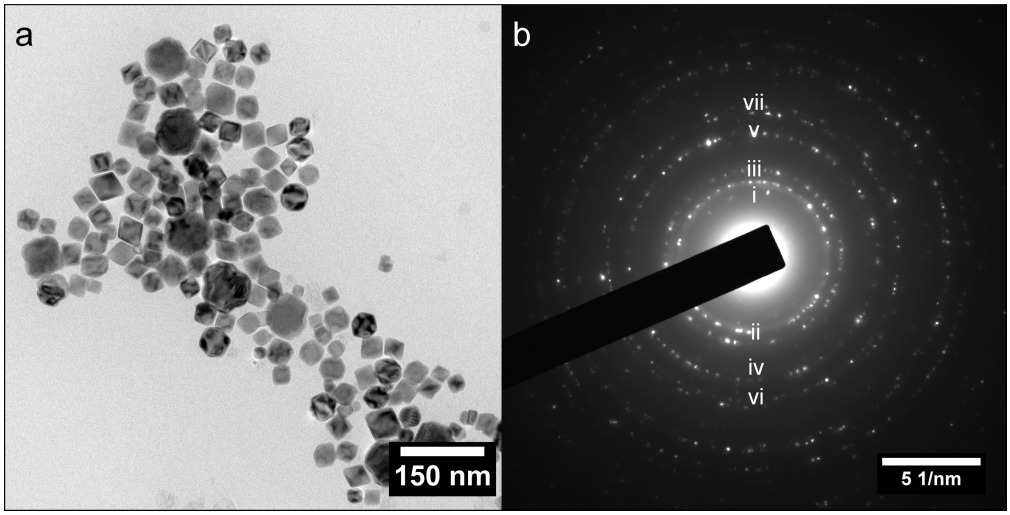

Figure S2 – (a) TEM micrograph of nanoparticles produced when no oleylamine is present in the reaction solution and oleic acid concentration is decreased with (b) the corresponding SAED pattern. The measured planar spacings correspond to wüstite[1] (FeO), magnetite[2] (Fe_3O_4) and/or maghemite[3] (γ-Fe_2O_3) as summarised in Table S4.

Table S4 – Planar spacings measured from SAED pattern in Figure S2.

SAED Figure S2(b) label	SAED planar spacings (Å)	Planar spacings for Wüstite[1] (FeO) JCPDS No. 46-1412	Planar spacings for Magnetite[2] (Fe_3O_4) JCPDS No. 19-629	Planar spacings for Maghemite[3] (γ-Fe_2O_3) JCPDS No. 24-81
i	2.92	-	2.9684	2.9513
ii	2.49	2.4863	2.5314	2.5168
iii	2.14	2.1532	2.0989	2.0868
iv	1.59	-	1.6158	1.6065
v	1.52	1.5225	1.4842	1.4756
vi	1.30	1.2984	1.2803	1.273
vii	1.24	1.2432	1.2118	1.2048

Detailed characterisation of distorted cubic nanoparticles

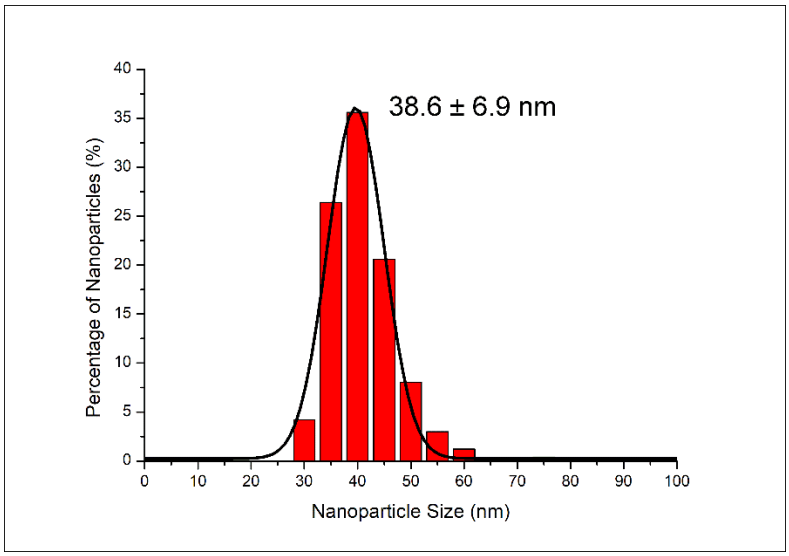

Figure S3 – Distorted cubic nanoparticles size distribution from bright field TEM imaging. 500 nanoparticles were used to determine the size (38.6 ± 6.9 nm).

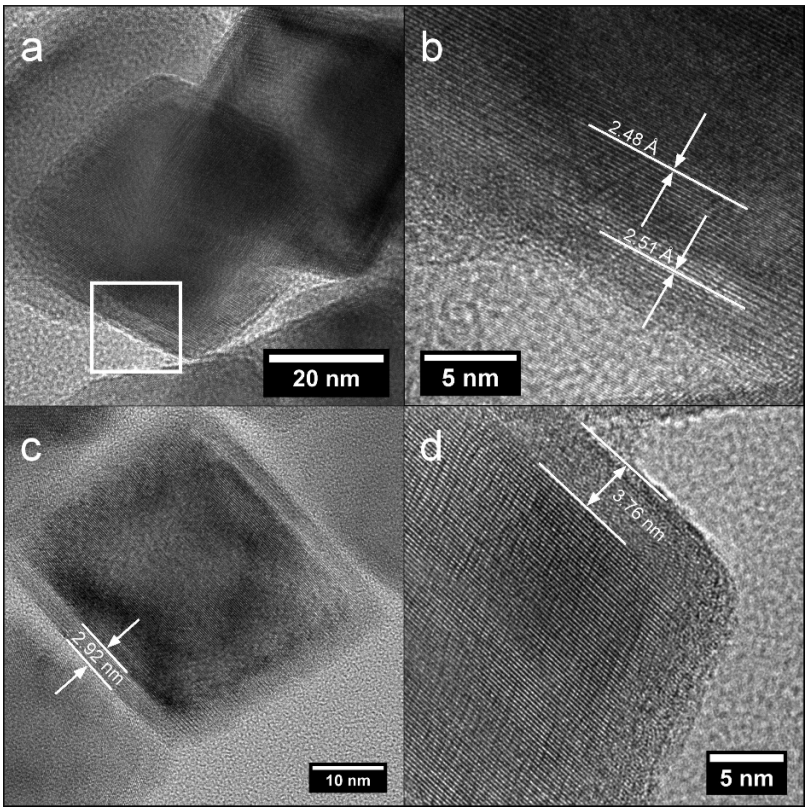

Figure S4 – Distorted cubic nanoparticles; (a) Nanoparticles with a selected area corresponding to (b) HRTEM lattice measurements are in agreement with the core consisting of wüstite (2.48 ± 0.03 Å) and the shell consist of magnetite/maghemite (2.51 ± 0.03 Å). (c) Freshly synthesised distorted cubic core-shell nanoparticle with a measured shell thickness of 2.92 nm and (d) cubic core-shell nanoparticle that has been aged for three months, with a shell thickness of 3.76 nm.

Table S5 – Planar spacings measured from SAED pattern in Figure 5.

SAED Figure S5(b) label	SAED planar spacings (Å)	Planar spacings for Wüstite[1] (FeO) JCPDS No. 46-1412	Planar spacings for Magnetite[2] (Fe_3O_4) JCPDS No. 19-629	Planar spacings for Maghemite[3] (γ-Fe_2O_3) JCPDS No. 24-81
i	2.949	-	2.9684	2.9513
ii	2.498	2.4863	2.5314	2.5168
iii	2.143	2.1532	2.0989	2.0868
iv	1.601	-	1.6158	1.6065
v	1.520	1.5225	1.4842	1.4756
vi	1.299	1.2984	1.2803	1.273
vii	1.249	1.2432	1.2118	1.2048

XRD of distorted cubic nanoparticles

Table S6 – XRD data summarised for the distorted cubic nanoparticles. Reflections correspond to magnetite[2] (Fe_3O_4) and/or maghemite[3] (γ-Fe_2O_3)), wüstite[1] (FeO), and iron[4] (α-Fe).

Position (°2θ)	Planar spacing (Å)	Relative Intensity (%)	Compound match	Miller Indices (hkl)
30.04	2.972	11.47	Fe_3O_4/γ-Fe_2O_3	220
35.42	2.532	39.35	Fe_3O_4/γ-Fe_2O_3	311
36.07	2.488	81.17	FeO	111
41.84	2.157	100.00	FeO	200
43.01	2.101	9.27	Fe_3O_4/γ-Fe_2O_3	400
44.62	2.029	9.02	Fe	110
53.43	1.713	3.86	Fe_3O_4/γ-Fe_2O_3	422
56.92	1.616	10.07	Fe_3O_4/γ-Fe_2O_3	511
60.74	1.524	47.59	FeO	220
62.48	1.485	15.29	Fe_3O_4/γ-Fe_2O_3	440
72.59	1.301	16.90	FeO	311
76.53	1.244	14.27	FeO	222

PDF card numbers for the phases presented in Table S6:

Fe_3O_4: JCPDS No. 19-629

γ-Fe_2O_3: JCPDS No. 24-81

FeO: JCPDS No. 46-1312

α-Fe: JCPDS No. 6-696

EDX Quantification

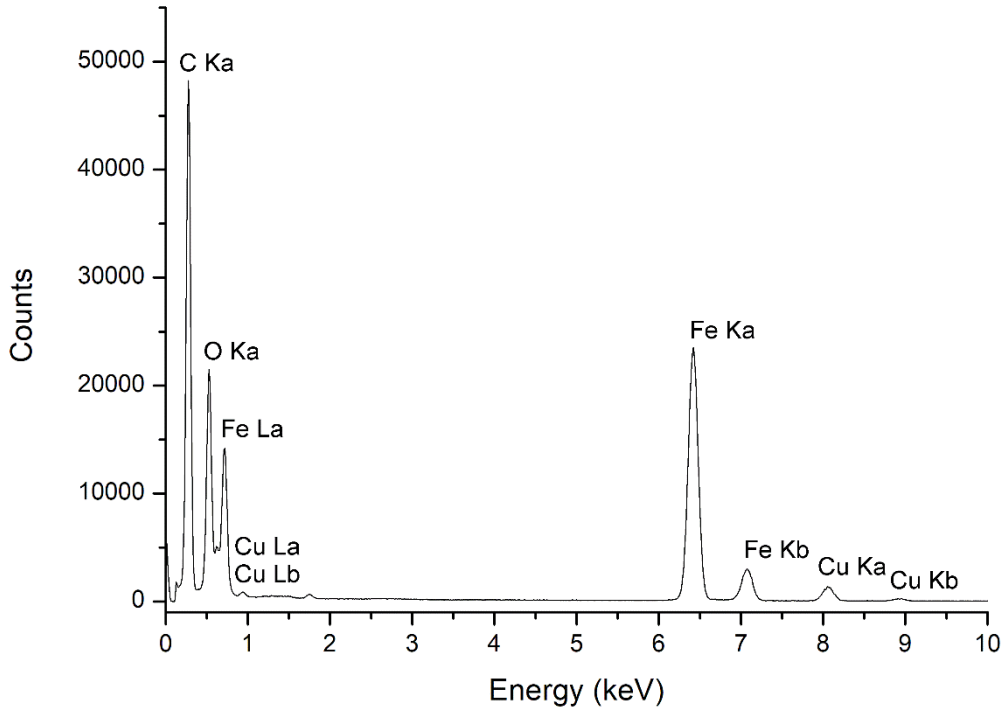

Figure S5 – EDX spectrum from centre of the distorted cubic particle in Figure 7.

Quantification of the EDX spectrum was carried out with Bruker's Esprit software using the Cliff-Lorimer model, confirming that the core of the particle has a Fe:O ratio close to 1:1, which further supports the conclusion that the NP core is wüstite, FeO (see Table S7, below).

Table S7 – Table with EDS quantification results

	Atomic Number	**Series**	**Concentration [wt. %]**	**Concentration [at. %]**	**Error (3 sigma) [wt. %]**
Iron	26	K-series	78.37	50.94	7.14
Oxygen	8	K-series	21.63	49.06	2.03
		Total:	100	100	

Extended reaction times

Table S8 – Planar spacings measured from SAED pattern in Figure 9(b).

SAED Figure 9(b) label	SAED planar spacings (Å)	Planar spacings for Wüstite[1] (FeO) JCPDS No. 46-1412	Planar spacings for Magnetite[2] (Fe_3O_4) JCPDS No. 19-629	Planar spacings for Maghemite[3] (γ-Fe_2O_3) JCPDS No. 24-81
i	2.88	-	2.9684	2.9513
ii	2.51	2.4863	2.5314	2.5168
iii	2.14	2.1532	2.0989	2.0868
iv	1.59	-	1.6158	1.6065
v	1.52	1.5225	1.4842	1.4756
vi	1.32	1.2984	1.2803	1.273
vii	1.27	1.2432	1.2118	1.2048

Exclusion of oleic acid from the reaction mixture

Ferrocene (0.26 M) was thermally decomposed in the presence of oleylamine (46 mM) as surfactant and 1-octadecene (20 mL) as solvent. Oleic acid was absent from the reaction mixture, similarly to previously reported literature.[5] The mixture was allowed to reflux under argon for an hour before being cooled to room temperature. The separation of nanoparticles from solution was challenging, as few nanoparticles appeared to form during this reaction. Unsurprisingly, the nanoparticles that did form (Figure S6) were smaller than the nanoparticles that formed when oleic acid was present in solution. These small nanoparticles also had some irregularity in regards to their shape. The average size of these nanoparticles was 5.00 ± 0.85 nm in diameter.

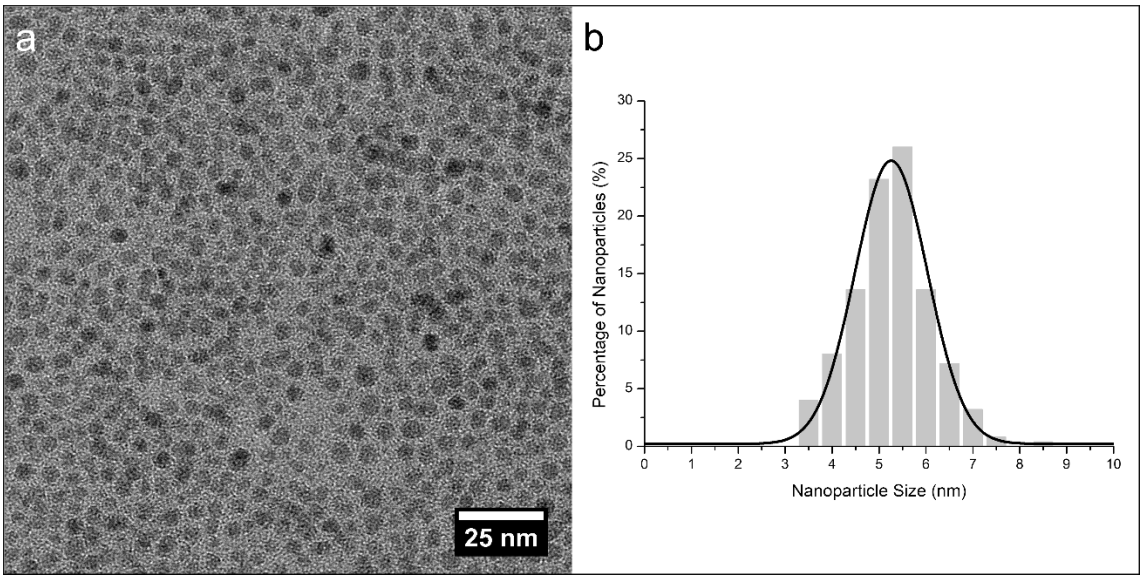

Figure S6 – Nanoparticles that formed (a) during the decomposition of ferrocene in the absence of oleic acid, with (b) accompanied size distribution from bright field TEM imaging. 250 nanoparticles were used to determine the size (5.00 ± 0.85 nm).

Distorted cubic nanoparticles with concave faces

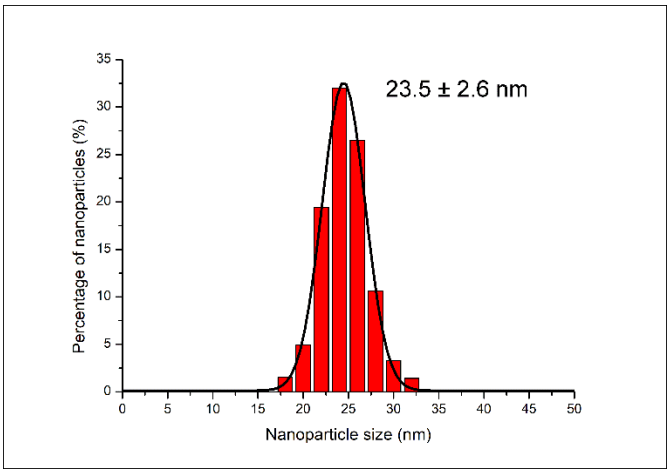

Figure S7 – Cubic nanoparticles with concave faces size distribution from bright field TEM imaging. 1000 nanoparticles were used to determine the size (23.5 ± 2.6 nm).

Table S9 – Planar spacings measured from SAED pattern in Figure 10(b).

SAED Figure 10(b) label	SAED planar spacings (Å)	Planar spacings for Wüstite[1] (FeO) JCPDS No. 46-1412	Planar spacings for Magnetite[2] (Fe_3O_4) JCPDS No. 19-629	Planar spacings for Maghemite[3] (γ-Fe_2O_3) JCPDS No. 24-81
i	2.98	-	2.9684	2.9513
ii	2.49	2.4863	2.5314	2.5168
iii	2.14	2.1532	2.0989	2.0868
iv	1.63	-	1.6158	1.6065
v	1.51	1.5225	1.4842	1.4756
vi	1.30	1.2984	1.2803	1.273
vii	1.24	1.2432	1.2118	1.2048

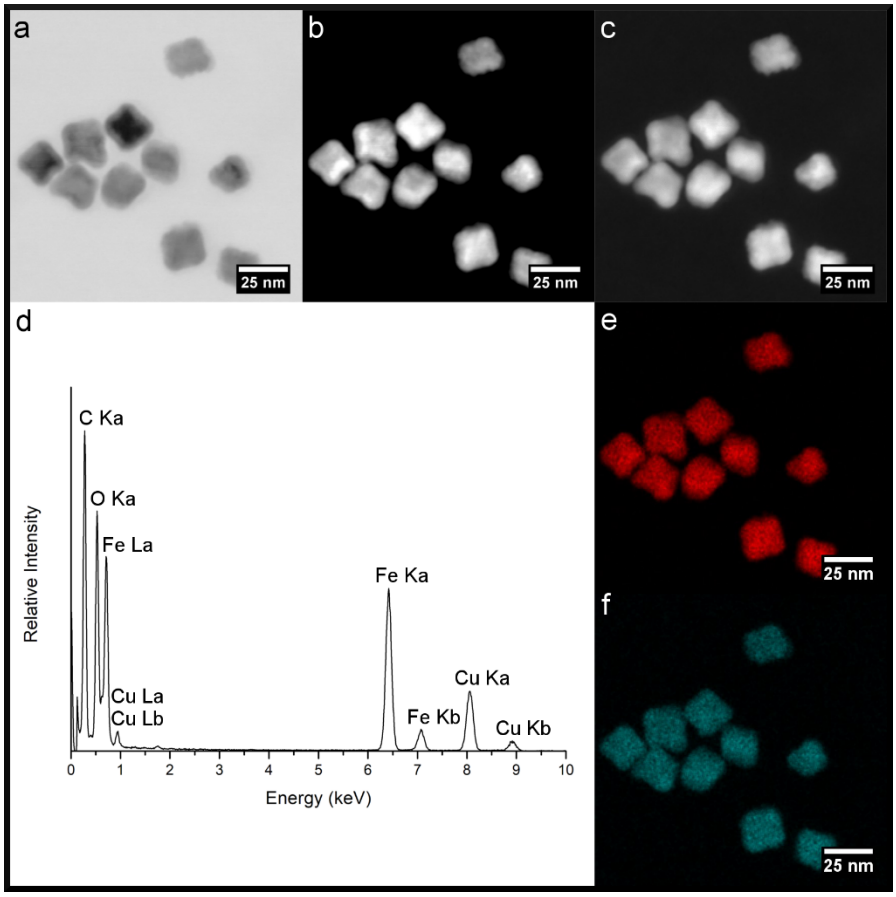

Figure S8 – STEM imaging of the cubic nanoparticles with concave faces. (a) BF STEM, (b) ADF STEM, and (c) HAADF STEM images suggest particles have a core-shell morphology. The EDX spectrum (d) showed the particles consisted of Fe and O, with Cu and C signals also observed due to the TEM grid. Elemental mapping shows the particles consisted entirely of (e) Fe and (f) O.

Extended reaction resulting in larger cubic nanoparticles with concave faces

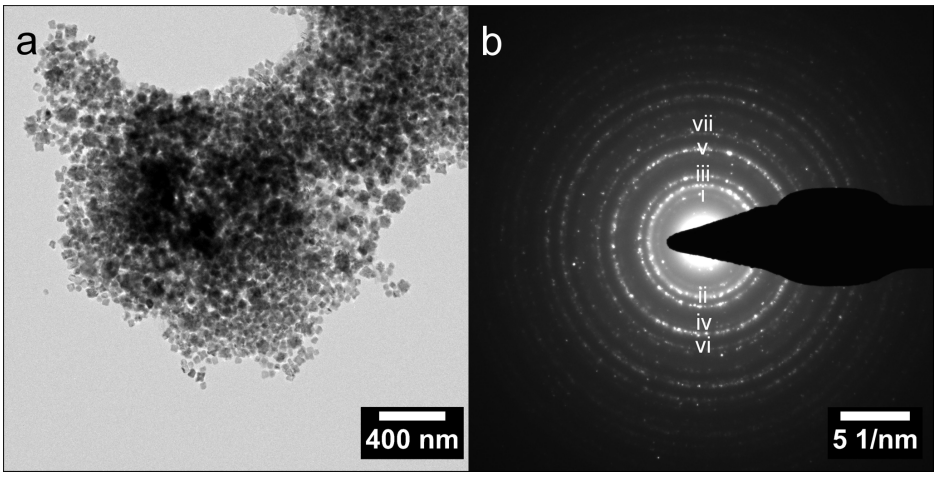

Figure S9 – TEM images of (a) larger distorted cubic nanoparticles with concave faces with corresponding (b) SAED. The measured planar spacings correspond to wüstite[1] (FeO), magnetite[2] (Fe_3O_4) and/or maghemite[3] (γ-Fe_2O_3) as summarised in Table S10.

Table S10 – Planar spacings measured from SAED pattern in Figure S9(b).

SAED Figure S10(b) label	SAED planar spacings (Å)	Planar spacings for Wüstite[1] (FeO) JCPDS No. 46-1412	Planar spacings for Magnetite[2] (Fe_3O_4) JCPDS No. 19-629	Planar spacings for Maghemite[3] (γ-Fe_2O_3) JCPDS No. 24-81
i	2.943	-	2.9684	2.9513
ii	2.489	2.4863	2.5314	2.5168
iii	2.141	2.1532	2.0989	2.0868
iv	1.611	-	1.6158	1.6065
v	1.515	1.5225	1.4842	1.4756
vi	1.303	1.2984	1.2803	1.273
vii	1.244	1.2432	1.2118	1.2048

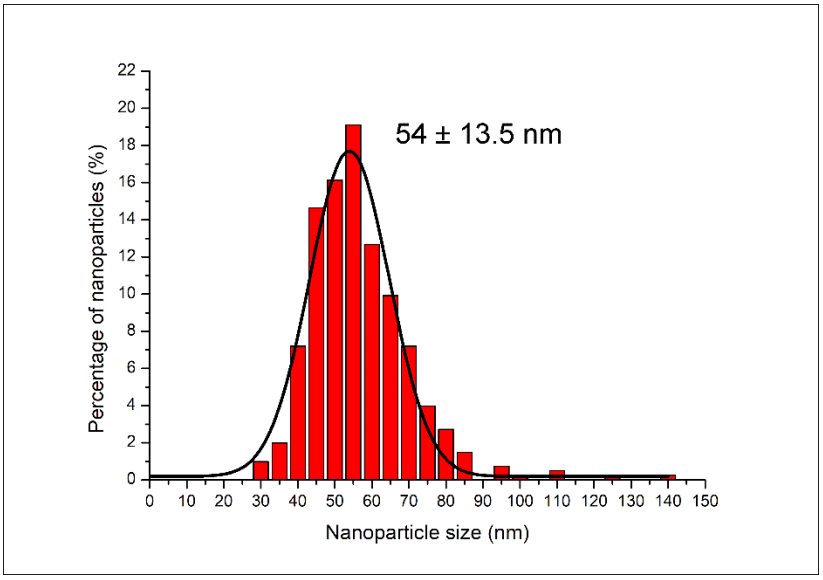

Figure S10 – Nanoparticle size distribution, from bright field TEM imaging, of the larger distorted cubic nanoparticles with concave faces. 400 nanoparticles were used to determine the size (54 ± 13.5 nm).

NMR experiments

^{1}H NMR experiment

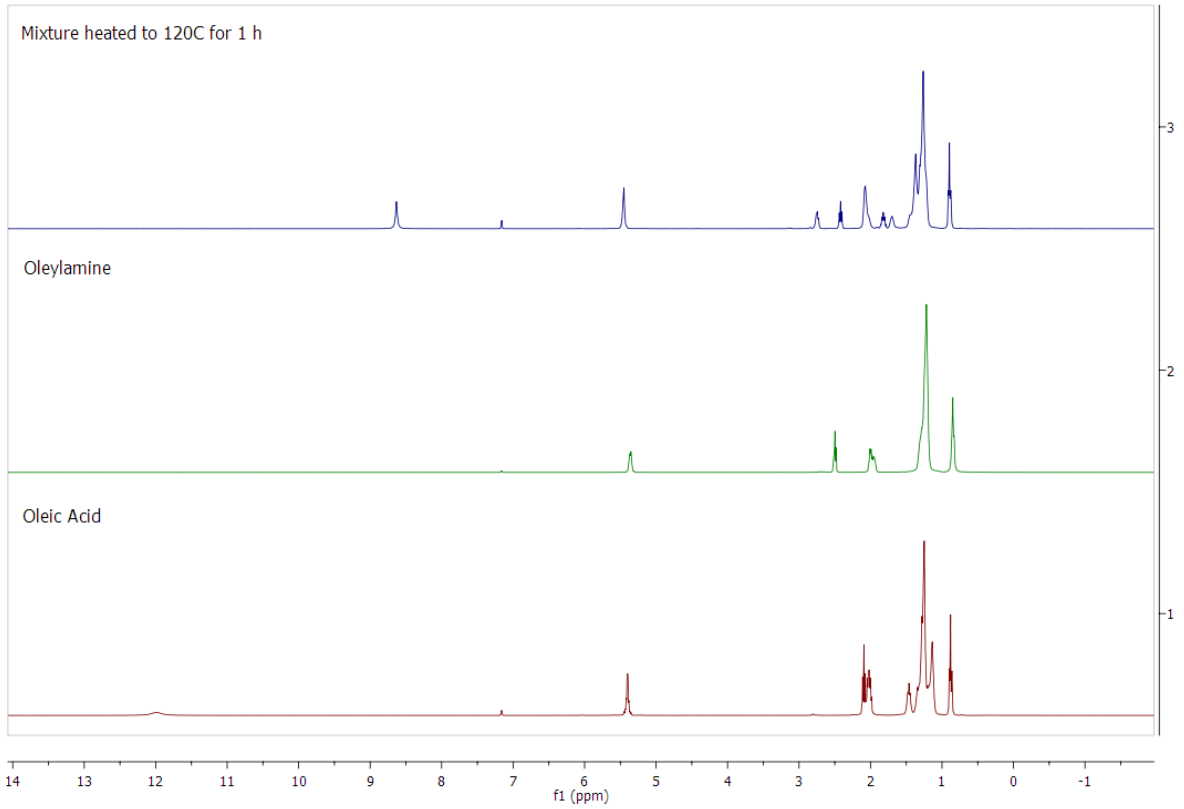

Figure S11 – ^{1}H NMR spectra of oleic acid, oleylamine and the surfactant mix after heating for 1 h. The most noteworthy feature of the NMR spectrum of the mixture is the appearance of a singlet peak at 8.63 ppm in the surfactant mix. This is indicative of a deprotonation of oleic acid and protonation of oleylamine. When integrating the peaks in the mixture spectrum the relative integrals of the peaks at 1.10 ppm, 5.55 ppm and 8.63 ppm were 6:4:3, which is consistent with a total of six protons on the two -CH_3 groups, four protons across the two double bonds and three protons on the –NH_3^+ functional group.

^{13}C NMR experiment

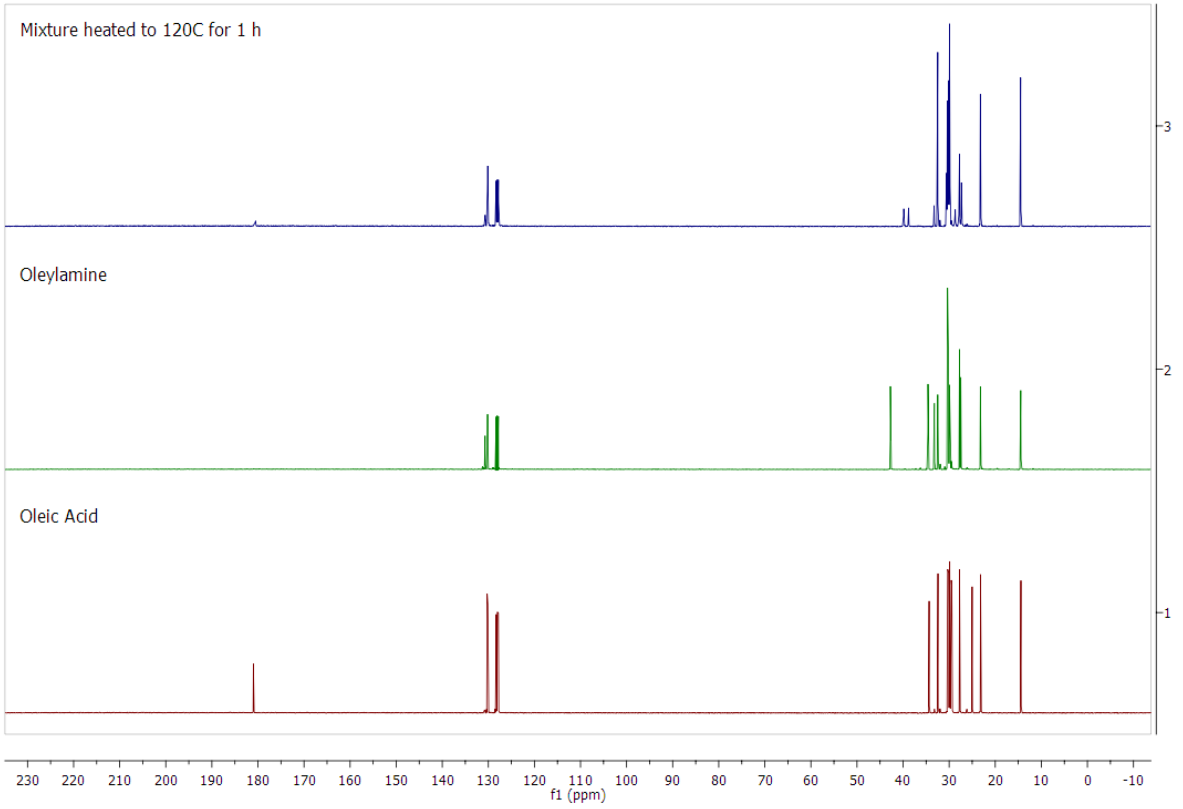

Figure S12 – ^{13}C NMR spectra of oleic acid, oleylamine and the surfactant mix after heating for 1 h. The most noteworthy features in the NMR spectra are the carbon peak at 180.99 ppm in the oleic acid spectrum is also apparent in the surfactant mix at 180.50 ppm. The peak at 42.75 ppm of the oleylamine spectrum appears to shift upfield to 39.85 ppm in the mixture spectrum, as oleylamine is protonated. The peak at 34.65 ppm in the oleic acid spectrum appears to shift downfield to 38.80 ppm in the mixture spectrum, as oleic acid is deprotonated. No new peaks consistent with an amide are present in the mixture spectrum.

References

1. H. Fjellvåg, F. Grønvold, S. Stølen and B. Hauback, *J. Solid State Chem.*, 1996, **124**, 52-57.
2. B. A. Welchsler, D. H. Lindsley and C. T. Prewitt, *Am. Mineral.*, 1984, **69**, 754-770.
3. A. N. Shmakov, G. N. Kryukova, S. V. Tsybulya, A. L. Chuvilin and L. P. Solovyeva, *J. Appl. Crystallogr.*, 1995, **28**, 141-145.
4. R. W. G. Wyckoff, *Crystal Structures - Volume 1*, Interscience Publishers, New York, 1963.
5. D. A. J. Herman, S. Cheong-Tilley, A. J. McGrath, B. F. P. McVey, M. Lein and R. D. Tilley, *Nanoscale*, 2015, **7**, 5951-5954.